COBEM 2023 27TH INTERNATIONAL CONGRESS OF MECHANICAL ENGENEERING

ABCM Brazilian Society of Mechanical Sciences and Engineering
27th ABCM International Congress of Mechanical Engineering
December 04-08, 2023, Florianópolis-SC, Brazil

COBEM-2023- 2088
PARAMETER ESTIMATION FOR DISCRETE ELEMENT METHODS (DEM) IN THE SIMULATION OF IRON ORE FLOW

José Cléber Rodrigues da Silva
Rogério José Marczak
UFRGS - Universidade Federal do Rio Grande do Sul
José Cléber <jcleberrsilva@gamil.com> , Rogerio Jose Marczak <rato@mecanica.ufrgs.br>

Abstract. *The discrete element method (DEM) has been increasingly used in flow simulation studies of granular materials in mining industry equipment (Classification, Comminution and Transport). This method consists of a computational technique that simulates the behavior of a granular material through the solution of particle motion equations, duly discretized and characterized by simulating the interaction between particles and geometries. For a closer to real characterization of the behavior of the flow of granulated materials, it is necessary to obtain input parameters (Coefficient of static friction, Coefficient of restitution, Coefficient of rolling friction), and the properties and mechanical characteristics of both. particles and geometries (specific mass, Poisson's ratio, shear modulus). Therefore, it is necessary to obtain these parameters through calibration methods. To date, there is no specific technical standard for applying this calibration, therefore, this article proposes to present a methodology for calibrating parameters, using iron ore as granulated material (Friable Hematite, "Canga" Iron Ore and Jaspilite, with variation in humidity, silica, alumina and Mn percentages). Laboratory tests combined with flow analysis in real equipment are used for validation, in addition to computer simulation models to determine static angles of repose and comparisons with DEM simulations and flows in real equipment such as vibrating screens and chutes. transfer. In the calibration for a blend of 40% friable hematite and 60% ore yoke, angles of repose ranging from approximately 32º to 70º and internal friction coefficients in the order of 2.88 to 3.78 were obtained, among other parameters. With DEM simulations using the parameters raised and after improvements to the equipment, we can see a reduction in failures due to handling and classification problems, as in the case of the rollerscreen sieve where the reduction was around 91%, in the modes of crash failure and overload and an increase in MTBF, in the order of 95%. The application of this calibration method allows obtaining a set of more assertive parameters for DEM simulation models in iron ore handling equipment.*

Keywords: *DEM, Calibration, Iron Ore, failure, Rollerscreen.*

1. INTRODUCTION

DEM (Discrete Element Method) modeling is a numerical simulation technique that has been increasingly used in industry and engineering to predict the behavior of granular materials in various applications, including mineral processing. The Discrete Element Method, initially proposed by Cundall and Strack (1979) is a methodology used in the analysis of the behavior of granular materials that follows a numerical approach based on in this method, the forces involved in the dynamics of particles are modeled and included in the equations of the movement of a particle originating a system of coupled ordinary differential equations that are explicitly resolved over time (Carvalho, et al., 2022).

Still according to Carvalho, et al., (2022), particles of various shapes and sizes, such as ores with coarse granulometry or even food grains and pharmaceutical powders, have great relevance in different types of industries. In pioneering work on DEM, Cundall and Strack (1979) proposed that two particles in contact overlap slightly. They proposed repulsive forces in relation to the overlapping distance between particles. The fundamentals of modeling conceptualized by these authors have been widely accepted by the scientific community and the contact laws of the semi-rigid sphere have been improved by several authors since their inception.

The increase in computational resources, favored the increasing use of DEM simulations that became more popular, both in industry and in academia and research centers, giving rise to the emergence of commercial software, such as Altair® EDEM™, Rocky DEM (ESSS®), Bulk Flow Analyst (Overland Conveyor®) and several free software such as LIGGTHS, applied by Jahani et al., (2015), Kratos Multiphysics (CIMNE - International Center for Numerical Methods in Engineering), YadeDEM , between others. Simulations with the DEM approach of semi-rigid particles using thousands of particles proved that they can coherently and efficiently model the behavior of granular and particulate materials (Carvalho, et al., 2022).

Granular materials are characterized by complex and variable properties, such as size, shape, hardness and friction, which directly influence the behavior of these materials during processing. Therefore, the calibration of DEM parameters is a fundamental process to guarantee simulation accuracy and, consequently, decision making in the design and operation

of iron ore beneficiation processes. The main DEM parameters that affect the iron ore simulation include particle interaction strength, static and dynamic friction, and modulus of elasticity.

Proper calibration of the set of parameters that define the interaction strength between particles is influenced by the geometry and properties of the particles' surfaces. Several authors have shown that the selection of contact force parameters must be made taking into account the particle size distribution and shape, in addition to considering the static and dynamic friction coefficient under different pressure conditions (Delaney et al., 2019; Zhao et al., 2020).

On the other hand, regarding the modulus of elasticity of the contacts, which is a measure of the stiffness of the interaction between the particles, it is important to adjust it properly based on the characteristics of the granular material, as highlighted by several works (Kiani et al., 2017; Li et al., 2018). Friction is another important factor in iron ore simulation using DEM, which can affect pile stability, flow rate and process efficiency. An adequate coefficient of friction depends on the contact surface, which can be affected by roughness, humidity and other environmental factors (Li et al., 2018; Zhao et al., 2020). Therefore, it is important to characterize the influence of these parameters under different operating conditions.

The modulus of elasticity is a measure of the stiffness of the granular material, it is another important factor in predicting deformations under different load conditions. For example, Kiani et al. (2017) highlighted the importance of adjusting the modulus of elasticity to simulate iron ore compaction during transport on conveyor belts. Both material density and moisture affect modulus of elasticity, and it is important to characterize these properties to ensure accurate calibration of parameters.

To calibrate DEM parameters, several methods are used, including triaxial compression tests, particle image analysis, density and moisture measurement, among others. Delaney et al. (2019) performed triaxial compression tests on iron ore particles to characterize the contact force between particles and adjusted the contact force using a neural backpropagation model. Li et al. (2018) combined laboratory tests with DEM simulations to optimize friction and elastic modulus parameters.

In this way, to guarantee the reliability and efficiency of the simulation and, consequently, of the prototypes of the bulk handling and transport equipment projects, it is essential to carry out an adequate survey and calibration of the DEM parameters that can reproduce the real flow conditions as closely as possible.

In this context, for this study, the methodology used by Calderón et. al. (2021), which consists of applying an estimate of the angles of repose for iron ore (Sinter Feed and ROM (Rom of Mine), with mixtures of about 60% “Canga” Hematinic and 40% Friable Hematite and humidity variation between 9 to 12%, the characterized samples varied in percentages of Jaspilite, silica, alumina, and Mn). A comparison was made between the static repose angles of the flow and granular flow of models in DEM with the real flow in ore piles in the yards, chutes and sieves and granular tests in the laboratory at VALE Carajás. For DEM simulations, Rocky®-DEM and EDEM™ software were used.

In short, the static angle of repose is the largest angle that a pile or slope of ore heap of a given granular material makes with the horizontal plane without slippage occurring as more material is added to the pile. In (Góes Filho, 2008) it is mentioned that the angle of repose for iron ore varies between 30° and 50°.

For iron ore from the Carajás mineral complex to which variations in grades and composition of canga/hematite blends and increased moisture content, caused by the seasonality of rainfall and mine dynamics, these angles can vary from 38° to 70°.

For parameter calibration in DEM simulations, the same procedure as in the laboratory experiment was replicated. At the end of each simulation, the repose and drawdown angles are measured. Finally, these results are compared with those obtained in the granular flow test.

2. DISCRETE ELEMENT METHOD

The DEM Discrete Element Method is a numerical technique that calculates the translation and rotation of each particle within a given domain in a small-time interval (time step), using a temporal integration scheme. In this concept, one can see the similarity with the characteristics of a granular medium whose behavior is governed by the interaction between individual particles and their surroundings (Grima and Wypych, 2011).

According to Zhu et al. (2008), the two most common types of DEM are those that use the soft-particle approach and the other that use the hard-particle approach. The soft count concept was first developed by Cundal and Strack (1979), which uses interpenetration between particles as a measure of the deformation that produces a contact force. According to these authors, the soft particle approach allows working with multiple contacts, while the rigid particle method processes only one collision at a time and considers the collision to be instantaneous.

In DEM, the mechanical behavior of the global system is described by the movement of each particle and by the force and moment acting on each of the contacts. Newton's second law of motion, Eq. (1) and Eq. (2), provide the fundamental relationship for the translation and rotation movement of the particles (Potyondy and Cundall, 2004).

The Discrete Element Method uses an explicit numerical solution to describe the individual motion of particles according to the interaction between them (Zhu et al., 2008; Matos et al.,2017). For a particle *i* its translational and rotational motion are, respectively:

$$m_i \frac{dV_i}{d_t} = \sum_j F_{i,j}^c + \sum_k F_{i,j}^{nc} + F_i^f + F_i^g, \quad (1)$$

$$I_i \frac{d\omega_i}{d_t} = \sum_{j=1}^{k} M_{i,j}, \quad (2)$$

Where m_i and I_i are mass and moment of inertia, respectively. V_i and ω_i are translational and rotational speeds, respectively. $F^c_{i,j}$ is the contact force between particles i and j. $F^{nc}_{i,j}$ is the non-contact force between particles i and j. F^f_i is the force of interaction between particle i and the fluid. F^g_i is the gravitational force applied on particle i. By means of numerical solutions, the discrete element method models the individual behavior of each particle and predicts the group behavior of several particles.

2.1 Contact models used in DEM.

Figure 1 presents the classification of DEM models of the interaction force between particles by contact force and non-contact force.

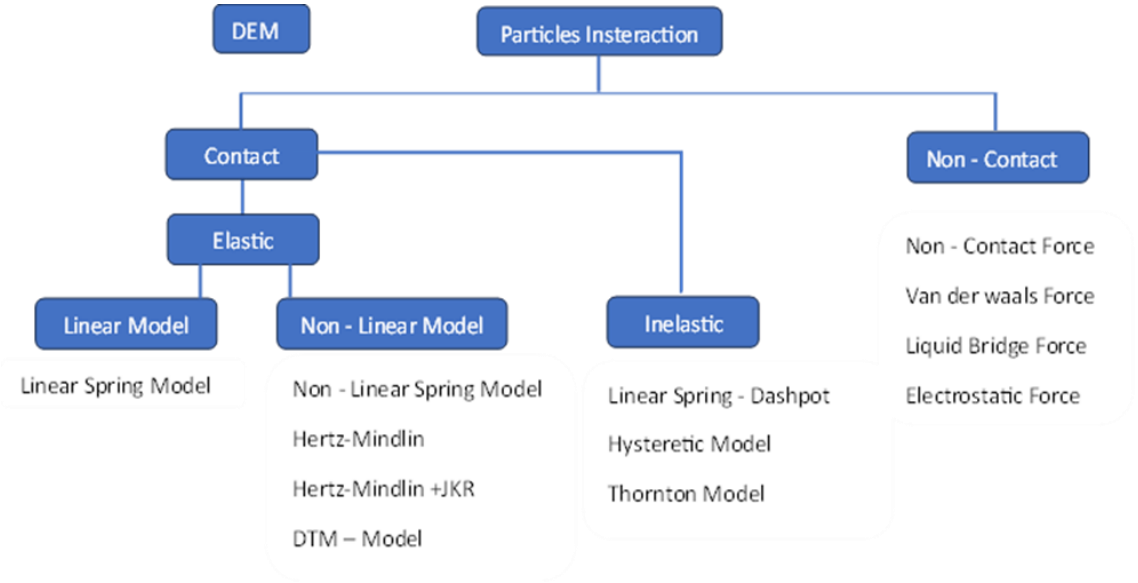

Figure. 1. Classification of force contact models between two particles (adapted from Murugesan, (2022)).

2.2 linear contact model

The linear contact model is widely used throughout the field of DEM and was first published in by Cundall, (1979). Normal force is a linear function of normal displacement (overlap); the shear force increases linearly with relative shear displacement but is limited by linear Coulomb friction. The graph in figure 02 presents the representation of the displacement curve versus the linear contact force. Equations 3 and 4 are the equations for the normal and tangential forces respectively.

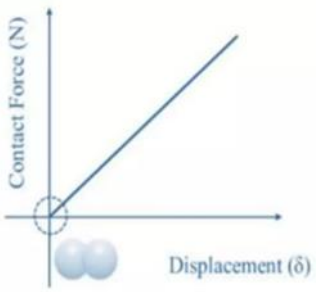

Figure. 2. Graph of the behavior of the linear elastic contact model between two particles (adapted from Murugesan, (2022)).

$$F_n = -k_n \delta_n, \quad (3)$$

$$F_t = -k_t \delta_t, \quad (4)$$

Where: F_n is the normal force; k_n is the Normal friction coefficient; δ_n is Normal displacement; F_t is the tangential force; k_t is the Tangential friction coefficient; δ_t is Tangential displacement.

2.3 Hertz-Mindlin contact model

The Hertz-Mindlin contact algorithm has been used to simulate the fall of microparticles and, thus, the generation of random packages as per (Machado, et. al., 2012). The basis behind the soft sphere model is that it allows two particles to deform during collision through an overlap. The superimposition allows the calculation of the frictional, plastic and elastic forces resulting from this collision as can be seen in the scheme of figure 3. The Hertz-Mindlin model describes the total force on each particle after the collision between particle *i* and particle *j* as follows as post by (Smuts, et. al., 2012).

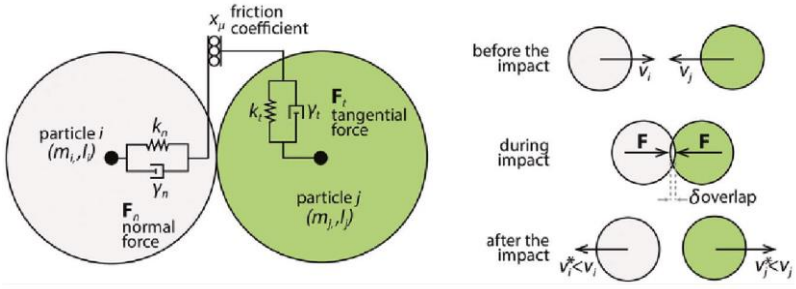

Figure. 3. Schematic of Hertz-Mindlin contact model between two particles (adapted from Capozzi et. al., (2019).

Therefore, we have some considerations about the Hertz-Mindlin contact model:

1. It is a non-linear elastic contact model;
2. Contact between two particles in the normal direction – Hertz Contact;
3. Models the contact between two particles in the tangential direction – Mindlin Theory
4. Hertz-Mindlin Model – Presents considerable complexity and computational effort, compared to the linear elastic model;
5. It has a simplification in the model as it does not model slip between particles – Hertz and Mindlin
6. Due to its precision, this model is widely used in the pharmaceutical industry.

Equations 5 and 6 present the mathematical model of normal and tangential forces.

$$F_n = -\frac{4}{3} E_{eq} \sqrt{R_{eq}} {\delta_n}^{3/2}, \tag{5}$$

$$F_t = 8 G_{eq} \sqrt{R_{eq} \delta_n \delta_t}, \tag{6}$$

Where: F_n is the normal force; δ_n is Normal displacement; F_t is the tangential force; k_t is the Tangential friction coefficient; δ_t is Tangential displacement; E_{eq} is the equivalent Young's Modulus; R_{eq} is the equivalent Radius Module; G_{eq} is the equivalent shear modulus.

The graph in Figure 4 shows the contact force curve as a function of displacement.

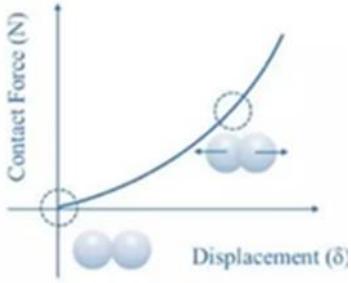

Figure. 4. Graph of the behavior of the linear elastic contact model between two particles (adapted from Murugesan, (2022)).

2.4 Hertz-Mindlin Contact Model + JKR Model

In DEM, The Hertz-Mindlin + JKR model describes this interaction between particles as follows:

1. Elastic Deformation (Hertz-Mindlin): When particles are close to each other, they undergo elastic deformation on their contact surfaces. This is modeled using the Hertz-Mindlin theory, which relates elastic deformation to applied force. The general Hertz-Mindlin relationship can be seen in equations 5 and 6.

2. Adhesion Force (JKR): In addition to elastic deformation, the JKR model considers the adhesion force that occurs due to intermolecular attractions on the contact surfaces. The Cohesive Particle Contact Model in adhesive theory uses a balance between the stored elastic energy and the loss of surface energy, presenting an opposing force due to the traction force. The JKR equation can be seen in equation 7.

$$F_{JKR} = \frac{4E_{eq}a^3}{3R_{eq}} - \sqrt{8\pi a^3 \Delta\gamma R_{eq}}, \quad (7)$$

Where: a is the contact area; γ is the surface energy; F_{JKR} is the adhesion force, R_{eq} is the adhesion force; $\Delta\gamma$ is the adhesive surface energy.

The graph in Figure 5 shows the contact force curve as a function of displacement of the Hertz-Mindlin + JKR contact model.

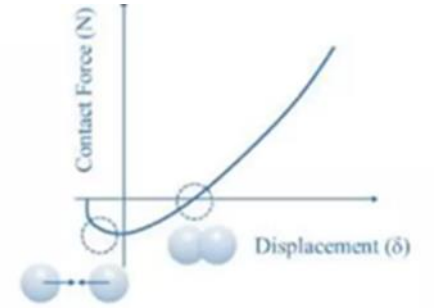

Figure. 5. Graph of the behavior of the linear elastic contact model between two particles (adapted from Murugesan, (2022)).

The total force between two particles in contact is the sum of the elastic force and the adhesion force and is presented in equation 7.

$$F_{total} = F_{elastic} + F_{adesão}, \quad (7)$$

2.5 Parameter Calibration - Discrete Element Method

Nasato (2011); Grima and Wypych (2009) express that there are some challenges in transforming a DEM analysis into a predictive tool, which include:

1. The development of efficient and valid methodologies to quantify and adjust DEM parameters;
2. Experimental validation of large-scale models to verify and establish techniques to apply DEM to modeling granular materials;
3. Development of scale-up techniques to adequately model the scale-up of equipment, without significantly affecting the quality of the results.

To model the behavior and achieve a granular behavior like real particulate matter in the desired application, Nasato (2011) states that several pilot-scale experiments can be carried out in order to make a "fine" adjustment of the DEM parameters, based on selected key parameters (e.g., particle shape and size distribution, solid density, contact stiffness, etc.). The objective of such calibration tests is to correlate the physical behavior of the particulate matter with the virtual behavior, with respect to its rolling motion, sliding motion, impact and restitution, and granular stiffness of the material, if relevant.

Just estimating parameters, such as the coefficient of restitution, cohesion, static friction and rolling friction, can be risky and reduces the reliability of the accuracy of the results if there is no experimental verification (GRIMA and WYPYCH, 2009).

The experiment to be used must be simple and quickly reproduced through DEM simulation, so that several simulations can be carried out of this experiment in a short period.

Also according to Nasato (2011), the method regularly adopted in the calibration stage is trial and error, and defines the steps to be followed, these are:

1. Measure experimentally or visually a given behavior;

2. Create a model in the DEM software that will reproduce behavior similar to that performed in the experimental test;
3. Feed the DEM model with a set of parameter values and run the simulation;
4. Check the results obtained with that set of values in order to verify how close the model is to the real behavior;
5. Return to the beginning of the simulation, modify one or more parameters and repeat the simulation; 6. Repeat steps 4 and 5 until you are satisfied that the correct parameters have been obtained.

A flowchart was created to demonstrate in a simplified way, the step-by-step methodology for calibrating DEM simulation models for any material, including iron ore. This methodology was defined in the work of Calderón et al. (2021), and adapted for this research, as well as in project simulation work in maintenance engineering at Vale's plants in Carajás (Serra Norte), This flowchart is presented in figure 6.

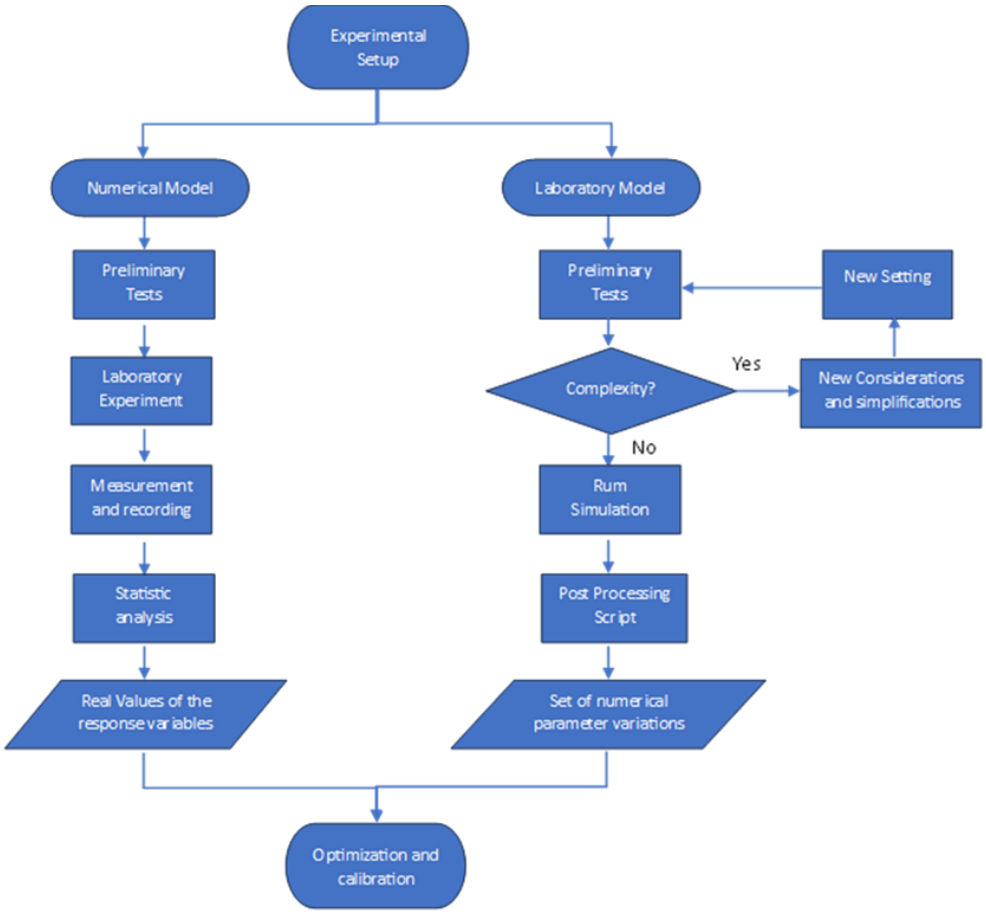

Figure 6. Second stage: development of laboratory experiment and DEM simulations (adapted from Calderón et al.,(2021)).

3. SUMULATION ROCKY DEM RESULTS

3.1 Simulation Conditions

In the DEM Rocky simulations, the same procedure as in the laboratory experiment is replicated. At the end of each simulation, the angles of repose are measured. Finally, these results are compared with those obtained in the granular flow test. When the results show differences below 5%, the parameters are considered calibrated. Two DEM analyzes were considered, one for friable hematite and the other with a blend of ore “Canga” Hematinic and friable hematite.

3.1.1 Data Simulation

Both in the experimental test and in the DEM simulation, constant environmental values of temperature and humidity were used. The density of friable hematite iron ore is indirectly calculated by the volume displaced in a test tube, resulting in a value equal to 2600 kg/m3, while for canga iron ore a value equal to 1720 kg/m3 was obtained with the same measurement method. The Chemical analysis, physical properties, granulometric distributions and materials interactions of the samples are presented in tables 01, 02, 03, 03, 05 and 06 respectively.

Table 1. Lithotypes Vs Chemical Contents for iron ore experiment.

Lithology	**Chemical Analysis (%)**								
	Fe	**SiO_2**	**P**	**Al_2O_3**	**Mn**	**TiO_2**	**CaO**	**MgO**	**PPC**
Hematite Friable (N4 Mine)	67.27	1.66	0.015	0.47	0.044	0.020	0.01	0.125	1.07
Hematite JP (N4 Mine)	66.99	1.06	0.013	0.70	0.16	0.039	0.014	0.056	2.15
Ore "Canga" (N4 Mine)	48.78	0.25	0.144	16.66	0.042	2.433	0.01	0.28	11.20

Table 2. Physics properties for iron ore experiment and DEM simulation.

Iron Ore Properties	**Iron Ore - Hematite**	**Ore "Canga"**	**Steel (Baundary)**
Density, (Kg/m^3))	2600	1720	7850
Young's Modulus, GPa	0.24	0.1	100.0
Poisson Modulus	0.3	0.27	0.3

Table 3. Size distribution for iron ore experiments and DEM simulation.

Size	**Iron Ore - Hematite**
32.5, mm	100%
30, mm	98%
27.5, mm	84%
25, mm	50%
22.5, mm	16%
20, mm	2%

Table 4. Size distribution for Blended iron ore of the experiments and DEM simulation.

Size	**Iron Ore - Hematite**	**Ore Canga**	**Ore Thick Canga**
50, mm	100%	100%	100%
40, mm	80%	72%	78%
20, mm	5%	40%	45%

Table 5. Materials Interactions to DEM single particles simulation.

Materials Interactions	**Static Friction**	**Dynamic Friction**	**Adhesive Distance (mm)**	**Restitution**
Particles to Particles (Hematite-Hematite)	0.99	0.98	1	0.3
Particles to Boundary (Hematite-Steel)	0,56	0,46	10	0.1

Table 6. Materials Interactions to DEM Blend simulation.

Materials Interactions	**Static Friction**	**Dynamic Friction**	**Adhesive Distance (mm)**	**Restitution**
Particles to Particles (Hematite-Hematite)	2.88	2.55	8	0.1
Particles to Boundary (Hematite-Steel)	0,56	0,46	10	0.1
Particles to Particles (Hematite - Canga)	3,78	2,88	8	0.1
Particles to Particles (Ore Canga)	0.3	0.3	0.1	0.3

3.1.2 Simulation Results

Next, the results of the DEM -Rocky simulations are presented, as well as the laboratory experiments and field observations. For the simulated parameters, the following angles of static repose were obtained.

Static angle of repose – SAOR - Static Angle of Repose: Iron Ore Hematite-Hematite -Simple Steel: Varying from 32.4° to 39.6°.

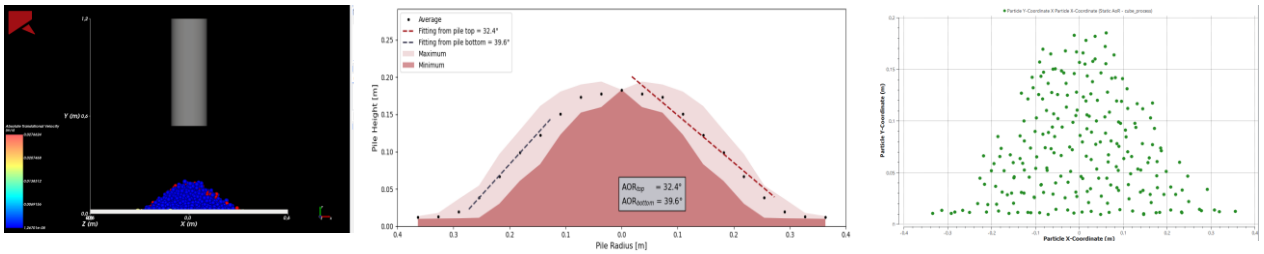

Figure 7. Simulation DEM-Rocky Hematite Friable(Author Himself.)

Static angle of repose SAOR - Static Angle of Repose: Blended Iron Ore Hematite-“Canga” -Simple Steel: Varying from 38.7° to 43.32°.

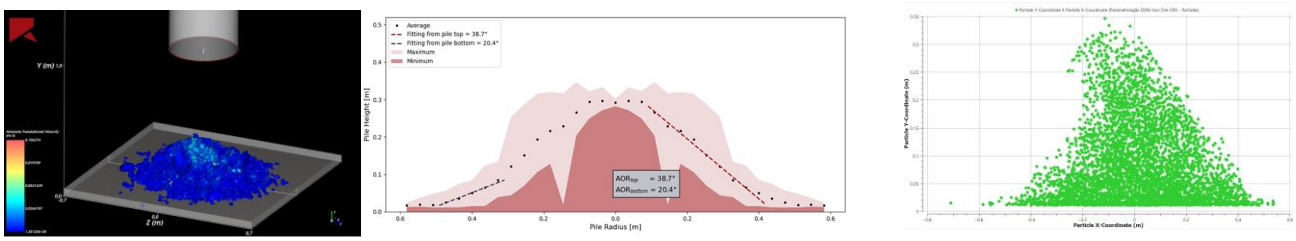

Figure 8. Simulation DEM-Rocky Blended Hematite and Ore” Canga”(Author Himself.).

Static angle of repose DAOR - Drained Angle of Repose: Blended Iron Ore Hematite-“Hematite” -Simple Steel: Varying from 47.07° to 55.5°.

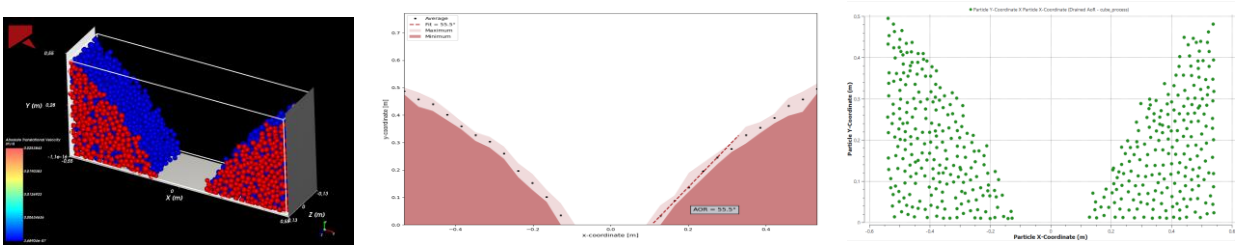

Figure 9. Simulation DEM-Rocky box slid method - Hematite Friable (Author Himself.).

Figures 10 and 11 present some laboratory tests to survey the static and dynamic angles of repose as well as siftability and mineralogical characterization tests for evaluation and cohesive analysis.

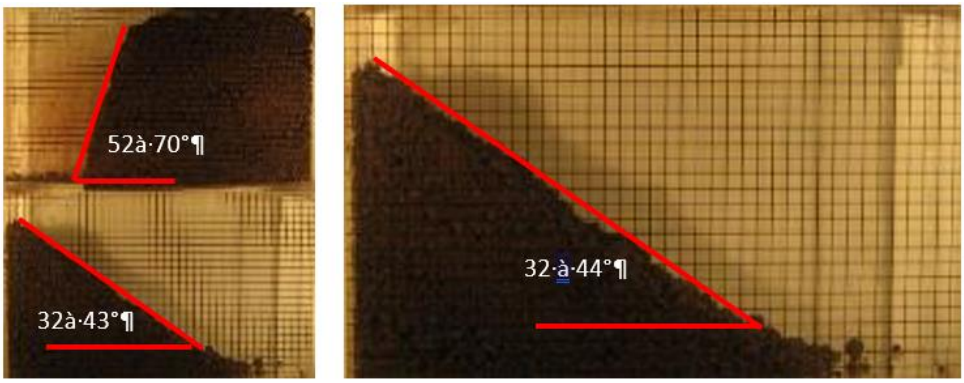

Figure 10 Ore Laboratory Experiment - Hematite 9 to 12% humidity (Vale, 2016)

Figure 11 Mineralogical characterization and siftability tests (Vale, 2020).

TML (Transportable Moisture Limit) tests were carried out on samples of goithitic and ferritic iron ores where the opinion of the mineralogy laboratory showed that, having found that the hydrated ore (Canga iron ore) with humidity above 9% has the characteristic of agglomeration due to free quartz and its association with silica. It makes transportation in treatment circuits difficult, reducing the production capacity factor. As can be seen in Figure 12.

Figure 12 Ore Laboratory Experiment - Hematite 9 to 12% humidity, TML Tests. (Vale, 2020).

3.1.3 Experiments Results and field observations.

Some field observations were carried out to obtain angles of the ore piles in the stockyards and transfer chutes. Some field observations were carried out to obtain angles of the ore piles in the stockyards and transfer chutes. Figures 13, 14 and 15 presented below show the angles of repose observed in the field under real flow conditions at Vale's plants in Carajás - PA - Brazil.

Figure 13. Piles of ore and chute observed in the field Vale iron ore plant in Carajás – Static angle of repose between 32° and 60°. (Vale, 2022).

Figure 14. Piles of ore observed in the field of Vale's iron ore plant in Carajás. Static angle of repose between 38° to 62°. (Vale, 2022).

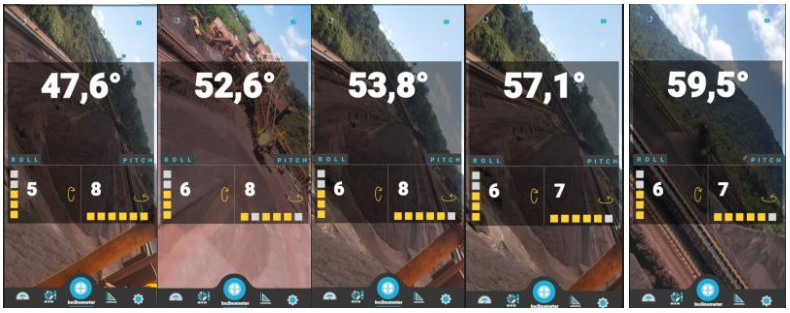

Figure 15. Piles of ore observed in the field of Vale's iron ore plant in Carajás. Static angle of repose between 32° to 62°. (Vale, 2022).

4. EXEMPLES OF EQUIPAMENTS SIMULATEDS

After the characterization and calibration tests of the DEM models, the standardization of parameters was carried out for the development of projects for roller screens, chutes and silos. In the analyses, iron ore was used as Sinter Feed and ROM, in the feeding and analysis of flows in hoppers, conveyor belt feed chutes, secondary crusher. Ensuring improvements in the flow of these equipment.

The following example presents the DEM simulation, with the parameters raised in this study, carried out to define the arrangement of the aligned discs for the Rollerscreem sieve and simulation of the flow profile and verification of sieving efficiency on a Single Deck 8x21 vibrating sieve in a secondary classification phase are presented in figure 16 a, b, c, and d respectively. The considerations and input data for simulations for improvements and new designs of Rollersreen type sieves were: Coarse hematinic hematite (“canga” ore), Fine hematinic hematite (“canga” ore) and Coarse friable hematite, Fine friable hematite. Material behaviors are different, as coarse materials do not interact as strongly as fine materials. Adjustment made to particle size distribution. Percentage of coarse particles distributed like this, Hematite 5% above 50mm; Canga ore 20% above 50mm; Mass distribution thus defined. 60% Canga; 40% Hematite. In this case, the interaction between coarse particles should not be considered, due to the weak interaction between them.

After carrying out the DEM studies and simulations, improvements were defined in the drive systems, discs and sieve shafts, which after their implementation, showed a significant reduction in failure modes and the number of locking and overload events in the order of 91% of reduction and increase in MTBF, around 95% and consequently in plant reliability, as can be seen in figures 17 and 18 respectively.

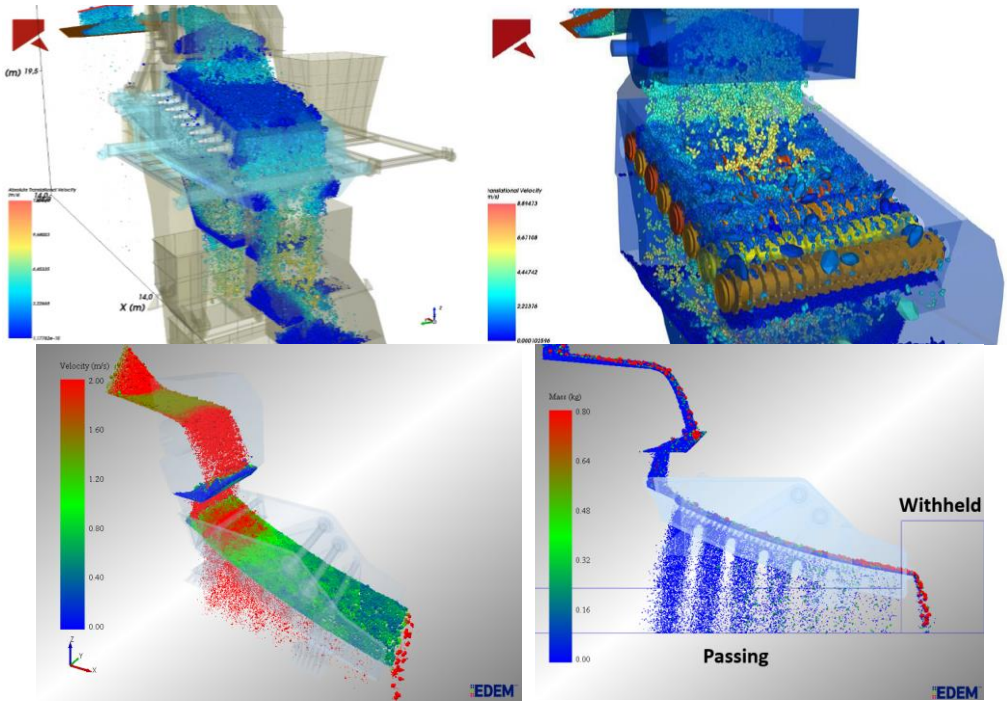

Figure 7 a ,b, c and d. DEM-Rocky and EDEM analysis for rollerscreen and vibrating screens. (Author Himself.)

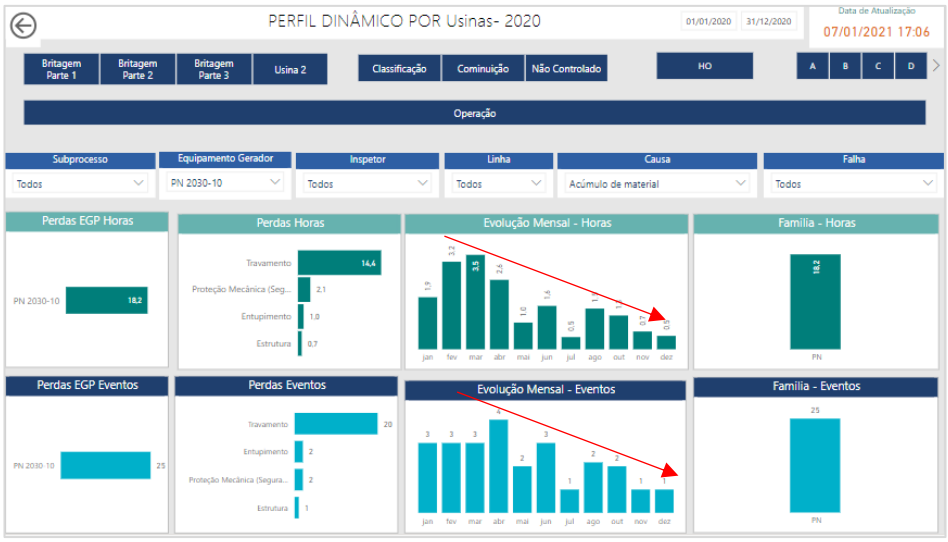

Figure 17. Loss profile of the PN-2030KN-10 in 2020 due to failures related to the locking of the Rollerscreen sieve shafts and discs, we see a tendency towards a reduction in failure modes (Vale, 202).

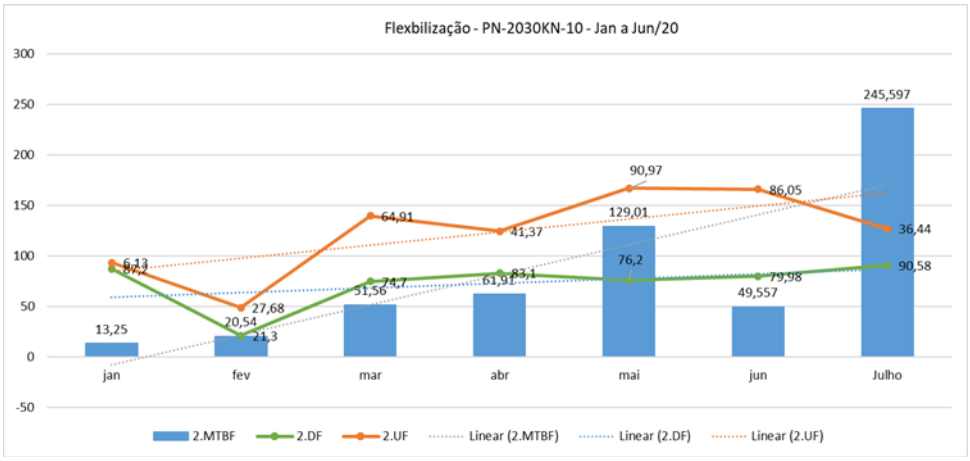

Figure 18. Physical availability, physical utilization and MTBF indicators of the PN-2030KN-10 in 2020 during the implementation of the improvements highlighted in the studies (Vale, 202)..

The following simulation in Rocky DEM was carried out using the parameters defined in this research, for the transfer chutes of the conveyors of the N4 mines and secondary crushing plants of plant 01 TR-113K-04, see (figure 19). This study was motivated by recurrent obstructions in the discharge chute when operating with ore blends above 60% ore yoke with high manganese. After simulation and re-engineering studies of the chute (design, manufacturing, and assembly) there was a reduction in recurrences of obstructions, as shown in the graphs in figure 20, where the reduction in failure modes related to obstruction of the discharge chute can be seen. TR-113K-04 in 2020.

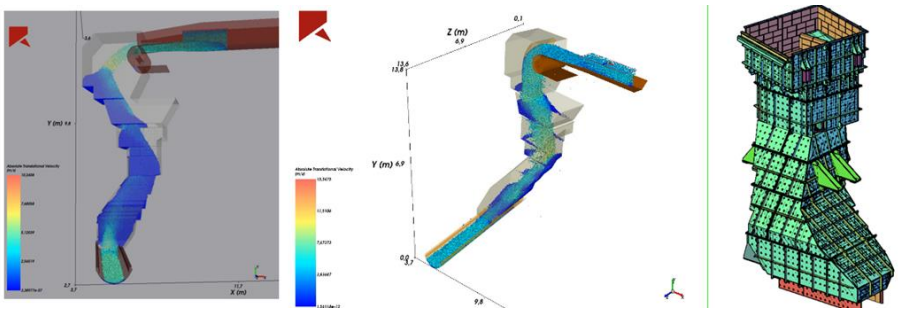

Figure 19. Rocky DEM analysis of flow in TR-113K-04 transfer chute. (Vale, 2020).

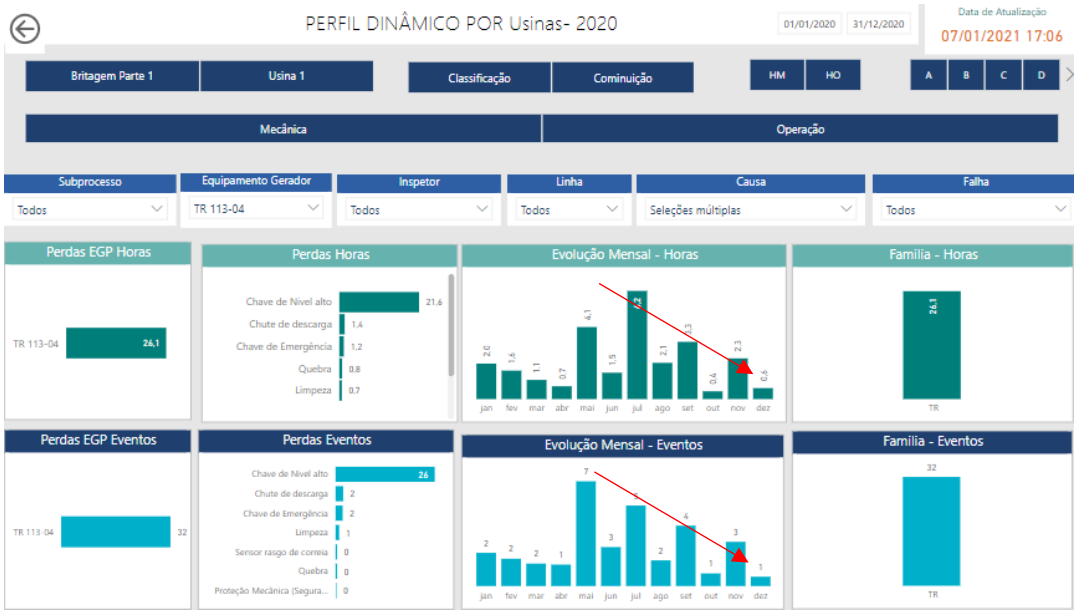

Figure 20. Loss profile of the TR-113K-04 in 2020 due to failures related to obstructions in the discharge chute, trend towards reduction in failure modes, (Vale, 2020).

This other example of DEM simulation presents, in addition to the flow, it includes the study of particle breakage and wear of the geometry for the Sizer type secondary roller crusher model MMD650, the objective of this study was to obtain the forces suffered by the teeth of the crusher shafts and define the best geometric profile and obtain the efforts in them as well as determine new wear materials with greater resistance to abrasion and shear see (Figure 21). In this case, a 50% reduction in the Sizer crusher's wear material consumption was captured, going from 14 to 07 changes after implementing the improvements highlighted by the DEM simulation study.

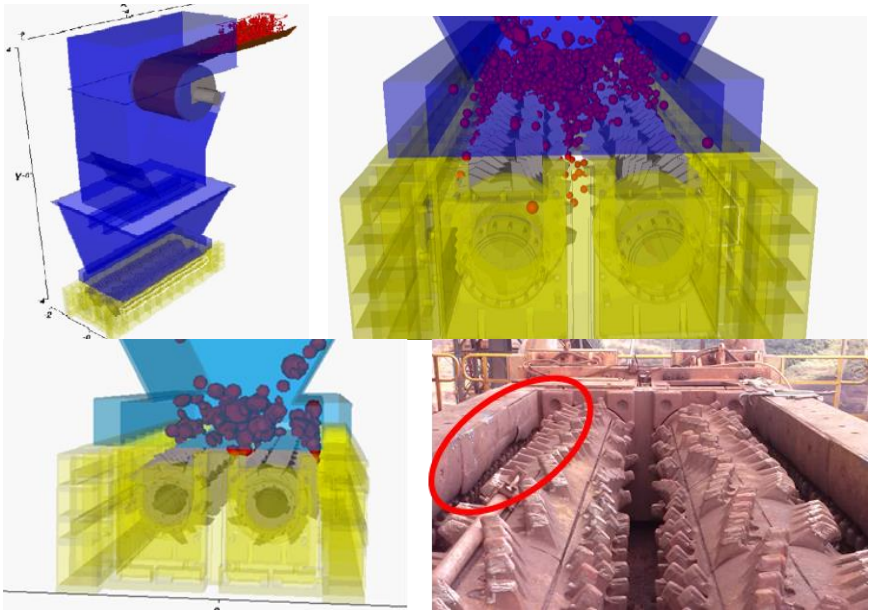

Figure 8. DEM-Rocky and EDEM analysis Sizer Crusher MMD650. (Vale, 2016).

5. CONCLUDING REMARKS

For this research, the methodology proposed by Calderón et al (2021) was implemented, where 3 (three) steps were defined and followed, with two types of models, experimental simulations and DEM, to survey and calibrate the parameters for iron ore, where these parameters were/will be used as standards for new studies and projects of transfer chutes, vibrating screens, Rollerscreens, among other equipment at Vale S/A's mineral processing unit in Carajás-PA, Brazil.

The first stage corresponded to the preparation of iron ore samples, sinter feed with friable hematite and ore yoke and the experimental procedure, where Vale's mineralogy laboratory and two Rocky-DEM simulation models were used. Step that establishes the basis for experimentation and research to collect data and define the calibration process.

In the second stage, laboratory experiments and Rocky-DEM simulations were carried out, references from calibration workshops 1 and 2 (SAOR - Static Angle of Repose and DAOR - Drained Angle of Repose, ESSS 2023).

And in the last step, the numerical parameters of the simulation are optimized, which best represent the behavior of the measurable variables in the experiment. In relation to the results of the calibration methodology proposed in this research, it is recommended for iron ore Friable Hematite, Canga de Ore and Blend, 60% Canga and 40% Hematite, which is the recommended blend configuration for transportation and handling in the production plant. processing. in the Carajás valley.

● Sintering feed flow - Iron ore, Hematite interaction with Hematite: value of 0.99 for coefficient of static friction, 1 millimeter for adhesive distance, 0.98 for rolling resistance and 0.1 coefficient of restitution

● Sinter Feed Flow - Iron Ore, Interaction of Hematite with Geometry (Smooth Metal): value of 0.56 for coefficient of static friction, 10 millimeters for adhesive distance, 0.46 for rolling resistance and 0.1 coefficient of refund.

● Flow rate of Sinter feed, Blend, 60% Canga and 40% Hematite, Hematite interaction with Canga: value of 3.78 for coefficient of static friction, 8 millimeters for adhesive distance, 2.88 for rolling resistance and 0.1 coefficient of refund.

It is worth mentioning that when applying the proposed methodology for calibrations, there was a high simulation time, due to the high number of tests necessary to validate the parameters and variables to be measured.

For future initiatives, new tests and calibrations can explore other levels, mixtures and materials, such as the handling of 100% “canga” with a high manganese content, because when this material enters the processing plant, transportation and classification (sieving) become more difficult, generating productivity losses and obstructions in the transfer chutes at various points in the process. Measuring the DEM parameters of these grades can restore new sizing of mineral processing equipment.

We can add that the methodology applied proved to be efficient in obtaining the parameters and using them as a standard, the final objective of this research, in the studies and projects of mineral processing equipment, proving its effectiveness. As can be seen in item 4.0 of this work, where simulations and graphs were presented with the reduction of failures (Obstruction, Blockages, accumulation of material) in the equipment (transfer chutes, Rollerscreen sieve and crushers) at Vale's processing plant in Carajás. The adoption of the new Rollerscreen sieve model, for example, reduced the active efforts on the shafts and bearings, by around 50% compared to the previous model, and this reduction was captured by the new DEM model. We can observe a significant reduction in failure modes and the number of crash and overload events of around 91% and an increase in MTBF, around 95%. Finally, we can conclude that DEM modeling is an efficient technique and strongly contributes to the design solutions for bulk handling machines and equipment, optimizing time and cost in the implementation of these projects.

6. ACKNOWLEDGEMENTS

We would like to thank VALE S/A, through Mr. Willian Pereira Martins for making available the laboratory and iron ore data contained in this work, thanks to ESSS, in the person of Marcelo Kruger for the technical support in the DEM Rocky simulations and personally to Vania Alves Donato for the support, crucial information in obtaining the data from DEM calibration in this project.

7. REFERENCES

Carvalho L. S. Análise De Modelos De Coesão Capilar Para Simulação De Fluxo De Materiais Granulares Aplicada Ao Manuseio Do Minério De Ferro // Dissertação de Mestrado. - Belém: Editora da Universidade Federal do Pará, 20 de Junho de 2013.

Cundall, P.A., Strack, O.D.L., 1979. A Discrete Numerical Model For Granular Assemblies. Geotechnique 29, 47–65.

Hertz, H., 1882. Uber Die Beruhrung Fester Elastischer Korper. Journal Fur Die Reine Und Angewandte Mathematik 92, 156–171.

Delaney, G.W., Morrison, R.D., Nordell, K.J., 2019. Calibration of Discrete Element Model Parameters for Iron Ore. Minerals Engineering 141, 105898.

ESSS. DEM technical manual - Version 2 0 2 3 R1.1. 6-30, 2023.

ESSS. Calibration 1: Static Angle of Repose. Updated for Rocky version 2023 R1, 4-24, 2023.

ESSS. Calibration 2: Drained Angle of Repose. Updated for Rocky version 2023 R1, 4-24, 2023.

Grima, A. P. Wypych, Investigation Into Calibration Of Discrete Element Model Parameters For Scale-Up And Validation Of Particle-Structure Interactions Under Impact Conditions, Powder Technol., 198 (2011).

Góes Filho, H.A. Planejamento Portuário. Vitória: [s.n], 2008. (Apostila da disciplina de Planejamento Portuário, Curso de pós graduação em engenharia portuária, UFRJ).

Kiani, R., Timperi, A., Brahma, S., 2017. On the Calibration of an Iron Ore Discrete Element Model and Predicting the Particle Breakage. Powder Technology 305, 111-126.

L. G. Calderón , R. E. Huidobro , S. Maggi. Experimental Calibration Methodology For Numerical Parameters In A DEM Software Based In Granular Material Static Tests. WMMES 2021, 2021.

Li, Z., Zakaria, M., Quang, T.V., Kisters, A., 2018. A Verification and Calibration Process for a DEM Model of Bulk Iron Ore. Powder Technology 329, 35-48.

Nasato, D.S. Desenvolvimento de Acoplamento Numérico entre o Método dos Elementos Discretos (DEM) e o Método dos Elementos Finitos. [Dissertação de Mestrado]. Faculdade de Engenharia Química, UNICAMP, Campinas, São Paulo; 2011.

M. Machado, P. Moreira, P. Flores, H.M. Lankarani, Compliant Contact Force Models In Multibody Dynamics: Evolution Of The Hertz Contact Theory, Mech. Mach. Theory 53 (2012) 99–121.

Matos, M., Lima, D.L., Mesquita, A. Calibração De Modelo De Partículas No Método Dos Elementos Discretos Usando Planejamento De Experimentos E Redes Neurais// XXVII Encontro Nacional de Tratamento de Minérios e Metalurgia Extrativa, Belém-PA, 23 a 27 de outubro 2017.

Mindlin, R.D., Deresiewicz, H., 1953. Elastic Spheres In Contact Under Varying Oblique Forces. Journal Of Applied Mechanics 20, 327–344.

Murugesan, Venkatasami. Presentation Discrete Element Methods., Tamil Nadu Agricultural University, 18-22, (2022).

Zhao, Z., Li, Y., Bao, G., Li, X., Tong, X., Wei, G., Xie, G., 2020. Calibration of the contact model parameters for discrete element modeling of iron ore sintering. Powder Technology 361, 177-189.

8. RESPONSIBILITY NOTICE

The author(s) is (are) the only responsible for the printed material included in this paper.